

Website publication 17 July 1998

NeuroReport 9, 2557–2563 (1998)

THE goal of this study was to determine the topographical and temporal specificity of neuronal and vascular responses using an intraoperative optical technique (iOIS). The face, thumb, index, and middle fingers were stimulated individually to obtain separate maps of cortical activation. Peak optical responses provided unique, non-overlapping cortical brain maps. Non-peak signals were more dispersed and produced overlapping responses from different digits. Peak iOIS responses colocalized with electrocortical stimulation mapping and evoked potentials. Temporally, we observed statistically significant specificity corresponding to sequential cortical activation during early optical signals (500–1750 ms), but later perfusion responses were non-specific. To our knowledge, this is the first report of either topographical specificity in overlapping spatial patterns, and/or temporal specificity in early perfusion profiles. These results therefore may have significant implications for other perfusion dependent functional imaging techniques. *NeuroReport* 9: 2557–2563 © 1998 Rapid Science Ltd.

Key words: Brain mapping; Cerebral blood flow; Human; Neurosurgery; Optical imaging; Vascular

Topographical and temporal specificity of human intraoperative optical intrinsic signals

Andrew F. Cannestra,^{1,3} Keith L. Black,²
Neil A. Martin,² Timothy Cloughesy,³
John S. Burton,^{1,3} Eduardo Rubinstein,⁴
Roger P. Woods^{1,3}
and Arthur W. Toga^{1,3,CA}

¹Laboratory of Neuro Imaging, ²Division of Neurosurgery, Department of Medicine, ³Department of Neurology and ⁴Department of Anesthesiology, UCLA School of Medicine, 710 Westwood Plaza, Los Angeles, CA 90095-1769, USA

CA,¹Corresponding Author and Address

Introduction

Functional activation studies in health and disease often depend upon perfusion related signals to localize the source of brain activity. Changes in functional perfusion form the basis for most modern functional neuro-imaging techniques including functional magnetic resonance imaging (fMRI),¹ positron emission tomography (PET),² optical imaging of intrinsic signals (OIS),³ near infra-red spectroscopy (NIRS),⁴ trans-cranial Doppler ultrasonography (TCD),⁵ and laser Doppler flow (LDF).⁶ These methods assume tight coupling between perfusion and neuronal activity. The full characterization of these activity-dependent perfusion related signals is therefore critical to understand and quantify brain activity. Currently however, most non-invasive human functional mapping techniques are resolution limited by low signal-to-noise ratios, long integration times or uncertain signal etiology. Additionally, research using most intraoperative functional mapping techniques (such as somatosensory evoked potentials (SSEPs), cortical evoked potentials (EPs), and direct cortical electrical stimulation (ESM), is often restricted by sampling and subsequent interpolation. Initial studies using optical intrinsic

signal imaging (OIS) within the surgical setting offered promise of a new technique for intraoperative functional mapping that may overcome current resolution limitations thereby providing a robust data source for human brain mapping research.^{7–9} OIS currently offers the spatial (μm) and temporal (msec) resolution necessary to observe rapid and transient signal changes by measuring optically active processes indirectly coupled to neuronal firing, including changes in blood volume,^{10,11} cellular swelling,¹² hemoglobin concentrations¹³ and cytochrome activity.¹⁴

Haglund *et al.*⁷ first demonstrated the use of OIS for functional localization in humans. Using a glass plate to stabilize the movement of the brain, epileptiform afterdischarges were observed in response to bipolar cortical stimulation over motor, premotor and somatosensory cortex. Functional activity also was observed during language tasks in Broca's and Wernicke's area. Toga *et al.*⁸ reported the first non-contact measurements of peripherally induced intrinsic signals during an intraoperative human study. Motor and somatosensory cortices were identified, and regional mapping of differential nerve stimulations characterized. Co-localization of OIS and evoked potentials in humans has been reported

by both Haglund *et al.*⁷ and Toga *et al.*⁸ Cannestra *et al.*⁹ recently characterized optical responses in rodent and human somatosensory cortex, describing temporal profiles in good agreement with other methods measuring vascular response.^{5,15,16}

The sensorimotor cortex in humans contains somatotopic functional architecture.¹⁷ Although this architecture is well established, little is known regarding the specific morphology of individual cortical representations. In previous studies we reported OIS temporal response with resolution near 1 s, and differential localization of median/ulnar nerve optical responses over somatosensory cortex.^{8,9} Building on these studies, we now investigate the temporal and topographic specificity of intraoperative optical intrinsic signals (iOIS) in sensorimotor cortex. Utilizing iOIS, SSEPs and ESM, we further examined the spatial and temporal relationship between perfusion and electrically based cortical representations.

Materials and Methods

Data acquisition: We measured optical reflectance changes over sensorimotor cortex in nine anesthetized patients undergoing surgical resection of fronto-parietal masses (tumors or arteriovenous malformations (AVMs)). Pre-surgical informed consent was obtained from all patients. The patient's head was fixed, via a Mayfield apparatus, to the operating table. After site localization (via a frameless stereotaxic system) craniotomy and reflection of the dura was performed.

SSEPs in response to median nerve stimulation were recorded to identify the location of the central sulcus. SSEPs were obtained from a 20 electrode cortical surface recording. Motor cortex was identified by a maximal amplitude negative peak. Somatosensory cortex was identified by phase reversal of the negative peak across the central sulcus where the negative end of the dipole was on the somatosensory cortex.¹⁸ Identification of pre- and post-central gyrus response foci facilitated subsequent optical imaging positioning and were correlated with the resulting optical signals. After SSEP recordings, the imaging system (camera, illumination and microscope) was positioned and stabilized. Before removal of the SSEP electrode grid from the cortical surface, an image was acquired to register SSEP and iOIS maps. Electrode dimensions and orientations were used to determine scaling and estimate cortical curvature.

The intraoperative optical imaging system utilized a slow scan CCD camera (model TE/CCD-576EFT, Princeton Instruments, Trenton, NJ) mounted via a

custom adapter onto the video monitor port of the Zeiss operating microscope. CCD camera response is linear over the light range collected. Similar methods were used as in previous publications.^{8,9} Images were acquired through a transmission filter at 610 (600–620) nm (Corion Corp., Holliston, MA). Circular polarizing filters were placed under the main objective of the operating microscope to reduce glare artifacts from the cortical surface. White light illumination was provided by the Zeiss operating microscope light source, through a fiber optic illuminator. Since the microscope view was determined by the surgeon's choice of magnifications and microscope placement, the experimental field of view (FOV) varied, depending on lens distance from cortex and specific orientation. FOV varied from 2.75 cm to 9.50 cm, resulting in spatial resolution of 100 μ m and 500 μ m, respectively.

iOIS acquisitions consisted of CCD exposure of the cortex during a control state (no stimulation) followed by a subsequent stimulated state (see below). Control trials and experimental trials were interleaved. Images were coregistered post-operatively utilizing non-linear automated image registration (AIR) algorithms^{19,20} implemented on a UNIX workstation.

Stimulations: During stimulation trials, baseline CCD images were acquired, then physiologically synchronized PC software triggered the stimulations (2s duration). Finger tip and cheek vibratory stimulations were administered using a custom built 110 Hz vibrator. Experiments contained 10–20 stimulation trials and included an equal number of non-stimulated interleaved controls.

Analysis: Optical reflectance images were analysed by pixel by pixel subtraction of a control trial and a stimulation trial. This subtracted image was then divided by the control image to normalize for differences between subjects and trials. These ratios thus represent proportional changes from baseline. Ratio images were averaged across trials at each time epoch to increase the signal-to-noise ratio (SNR). No other digital image processing was performed.

Signal magnitude was defined as the average pixel intensity in a statistically defined region of interest (ROI). ROIs were first created from the averaged ratio images at each time point by performing a three pixel Gaussian blur, equalizing and thresholding at the mean pixel value ± 1 s.d. This ROI was then superimposed upon the original averaged ratio image and the magnitude calculated. The time point with the largest calculated magnitude was considered to be the maximal optical response for the trial. In Fig. 1, this maximal ROI was then superimposed upon the other images of the trial to calculate the

respective magnitude at each time point. To compare between maps in Fig. 1, the total average intensity change for thumb, index, and middle finger maps was used for thresholding.

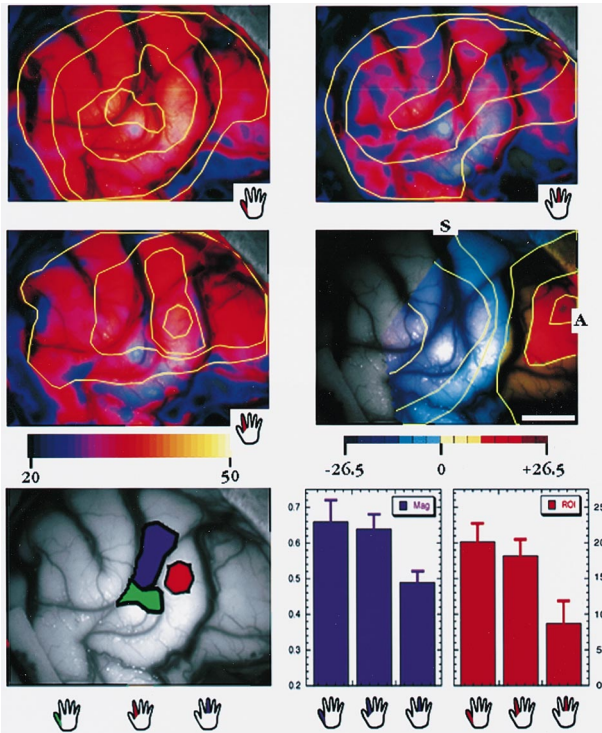


FIG. 1. Thumb, index and middle finger stimulations produced separate cortical activation maps (upper left, middle left and upper right, respectively). When the total average intensity change (for all images) was applied as threshold, the total optical response area (union all fingers combined) was 22.6 cm². Thumb optical response was largest at 20.0 cm² followed by index (18.0 cm²) and middle fingers (9.3 cm²). These finger response regions were contained within the functional map obtained by SSEP's (middle right). Thumb (green and yellow, lower left panel) localized more inferior than index finger response (red and yellow). Both thumb and index finger overlapping and thumb/index/middle finger overlap localized centrally within the SSEP map. Thumb and index finger responses activated motor cortex predominantly more than middle finger stimulation (as observed by the SSEP map). The orientation of individual digit responses in Fig. 1 is consistent with the classical homunculus schematic.¹⁷ When peak iOIS responses are displayed over somatosensory cortex, a superior to inferior orientation is revealed for the middle (purple), index finger (red) and thumb (green), respectively (lower left panel). The distances from the median nerve SSEP phase reversal (within the central sulcus) and maximal sensory iOIS responses are 10.7, 4.0, and 5.8 mm for thumb, index and middle finger, respectively. The bar graphs represent average intensity change per pixel (magnitude in units of reflectance change $\times 10^{-4}$) and cortical spatial involvement (ROI in cm²) for thumb, index, and middle fingers, respectively. Thumb and index finger vibration induced the largest optical response, comparable within standard deviations. Middle finger vibration induced a near 50% smaller optical response. Thumb and index finger activated with comparable intensities, while middle finger stimulations yielded a diffuse activation (25% magnitude difference). Middle left color bar indicates reflectance change $\times 10^{-4}$. OIS magnitude contours were obtained by tracing signals after a 5 pixel Gaussian blur. SSEP contours segregate changes in potential. Middle right color bar indicates mV potential. Images are from a single patient (10 stimulation trials for each stimulus location). Scale bar is 1 cm. Spatial resolution is 335 μ m/pixel. A, anterior; S, superior.

Results

Figure 1 describes spatial characteristics of cortical optical response. Thumb, index, and middle fingers were stimulated individually to obtain separate cortical activation maps. These finger response regions all were contained within the activation map obtained by median nerve transcutaneous stimulation SSEPs. Large regions of overlap were observed between individual finger responses, and localized centrally within the SSEP map. These regions (intersection of finger responses) comprised 15.7 cm² and 8.0 cm² for index/thumb and thumb/index/middle finger overlaps, respectively. The combined index/thumb optical spatial response closely correlated with median nerve SSEP activity (16.4 cm²). Index finger cortical response localized more superior than thumb representation. Thumb and index finger responses activated motor cortex more than middle finger stimulation. Thumb and index finger vibration induced the largest optical responses (spatial involvement) and were equivalent within s.d. Middle finger vibration induced a near 50% smaller optical response. Thumb and index finger activated with comparable intensities, while middle finger stimulations yielded a smaller, diffuse activation (25% smaller magnitude).

When maximal iOIS responses were examined over sensory cortex, middle, index and thumb representations were oriented superior to inferior. These peak iOIS responses existed within the -6.0 mV (and larger) potential of the transcutaneous electric median nerve representation. The distances from the median nerve SSEP phase reversal (within the central sulcus) and maximal sensory iOIS responses were 10.7, 4.0, and 5.8 mm for thumb, index, and middle finger, respectively.

Figure 2 describes the relationship between iOIS, EPs and ESM. The thumb and face (cheek) were stimulated individually to obtain separate iOIS maps. Thumb localized within the region demarcated by ESM and large potential changes. The cheek response was more inferior, consistent with the findings from ESM. Peak intensity iOIS responses accurately localized with stimulation sites. Thumb and facial responses activated large regions of motor cortex. Inferior post-central activation also was observed during facial stimulation, however was probably distorted due to the location of AVM.

The temporal specificity of human optical intrinsic signals is shown in Figs 3 and 4. Dividing the optical image along the central sulcus (identified by SSEP phase reversal at 20 ms) allowed separate analysis of motor and sensory signals. Within 500 ms post-stimulus, sensory responses increased to 30% over baseline, in contrast to only 10% over motor cortex (Fig. 3). Both intensity curves reached a maximum

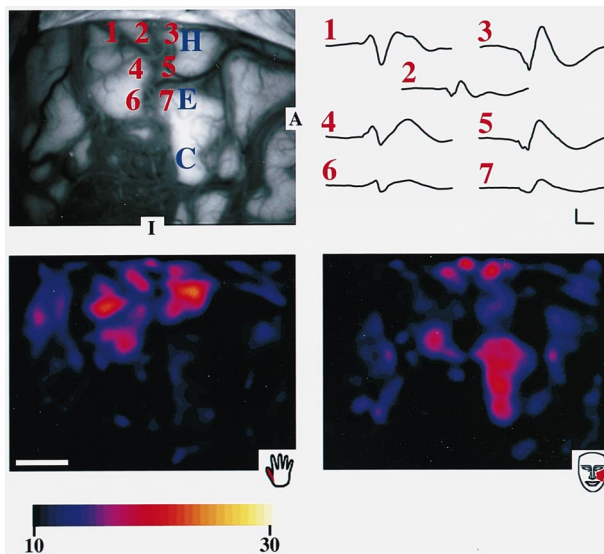


FIG. 2. Thumb, and facial (cheek) stimulations produced separate cortical activation maps (lower left, and lower right, respectively). These regions correlated with intraoperative mapping of cortical representations by electrocortical stimulation mapping (ESM; upper left, blue letters). Thumb also localized with large evoked potential changes observed from transcutaneous median nerve stimulation (traces, upper right; numbered locations, upper left). Thumb localized more superior than cheek response. Thumb and facial responses activated large regions of motor cortex. Inferior post-central activation is observed during facial stimulation, however is probably distorted due to the location of the arterial-venous malformation (AVM). Images are from a single patient. Scale bar is 1 cm. EP axes are $10 \mu\text{V}$ and 5 ms, respectively. The first peak in traces 1, 4 and 6 is the N-20 ms peak. Phase reversal across the central sulcus (in traces 3, 5, 7) is noted at P-23 ms. Trace 2 appears iso-electric. Spatial resolution is $500 \mu\text{m}/\text{pixel}$. Left color bar indicates reflectance change $\times 10^{-4}$. Images are from a single patient (10 stimulation trials for each stimulus location). A, anterior; I, inferior.

at 2.0 s and returned to baseline near 4 s. The intensity difference at 1.0 s was statistically significant ($p < 0.05$, one-sided), and approached significance ($p < 0.10$, one-sided) at 0.5 s. The motor and sensory response profiles did not differ after peak response.

Temporal specificity was also observed in the presence of large magnitude differences (Fig. 4). Images acquired with higher temporal resolution imaging (350 ms, Fig. 4) did not reveal responses earlier than 500 ms. Initial somatosensory responses were detected in the second post-stimulus image (at 700 ms). In contrast, detectable changes over motor cortex were not detected until 1.4 s. Sensory cortex response magnitude was near double motor cortex response. When normalized for this magnitude difference, somatosensory response also preceded motor cortex response. Sensory cortex response increased to 64% at 1.75 s, in contrast to 25% over motor cortex. As above, both intensity curves reached a maximum at 2.1 s and returned to baseline near 4 s. When normalized for peak intensity differences, the intensity difference at 1.05 s and 1.75 s was statistically significant ($p < 0.04$ and

$p < 0.01$, one-sided, respectively). After normalization the response profiles did not demonstrate temporal specificity after peak response.

Discussion

This study measured the dynamics and complexity of vascular and metabolic responses to a variety of stimuli. We found the responses to be spatially specific and sensitive to stimulus parameters. Regional evaluation of response profiles revealed temporal specificity during early perfusion responses.

Topographical specificity: The median nerve transcutaneous electrical SSEP response should encompass an area responsible for the thumb, index, middle, and portions of the ring finger.²¹ Our observations are consistent with such topography, demonstrating all finger (thumb, index, and middle) iOIS responses within the median nerve SSEP map. Electrocortical mapping has revealed lateral inferior to medial superior order of thumb, index and middle fingers with overlap or reversal for adjacent digits.²² Our iOIS finger maps confirm these electrocortical results. Additionally, the superior/inferior orientation of middle, index finger and thumb, and the small/diffuse representation of the middle finger, are consistent with the orientation of traditional homunculus representations.¹⁷ As shown in Fig. 1, cortical surface activations (thumb/index *vs* middle) differed by $\sim 50\%$, while signal intensity within these ROIs differed by 25%. The total area of response (union of all digits, 22.6 cm) is similar to areas reported by PET (22 cm)²³ and the size of the homunculus representation drawn by Penfield and Rasmussen.¹⁷ Peak perfusion-dependent responses produced comparable localizations to individual digit electrocortical studies.²⁴ Peak iOIS responses may, therefore, correlate with brain maps obtained by direct cortical stimulations¹⁷ and single dipole localizations in electrocortical studies.²⁴

iOIS localizations were consistent with cortical maps obtained by ESM mapping, and evoked potential measures (Fig. 2). The superior-inferior orientation of hand and face (from iOIS and ESM mapping) also is consistent with traditional homunculus representations.¹⁷ These results provide additional evidence that peak iOIS responses spatially co-localized with electrically defined cortical representations.

Close examination of magnitude contours in Fig. 1 reveals patterns of overlapping response. During thumb stimulation, the second peak contour encompasses the regions corresponding to peak activation for index and middle fingers. Similarly, during index finger stimulation, the second peak contour encompasses the cortical region corresponding to

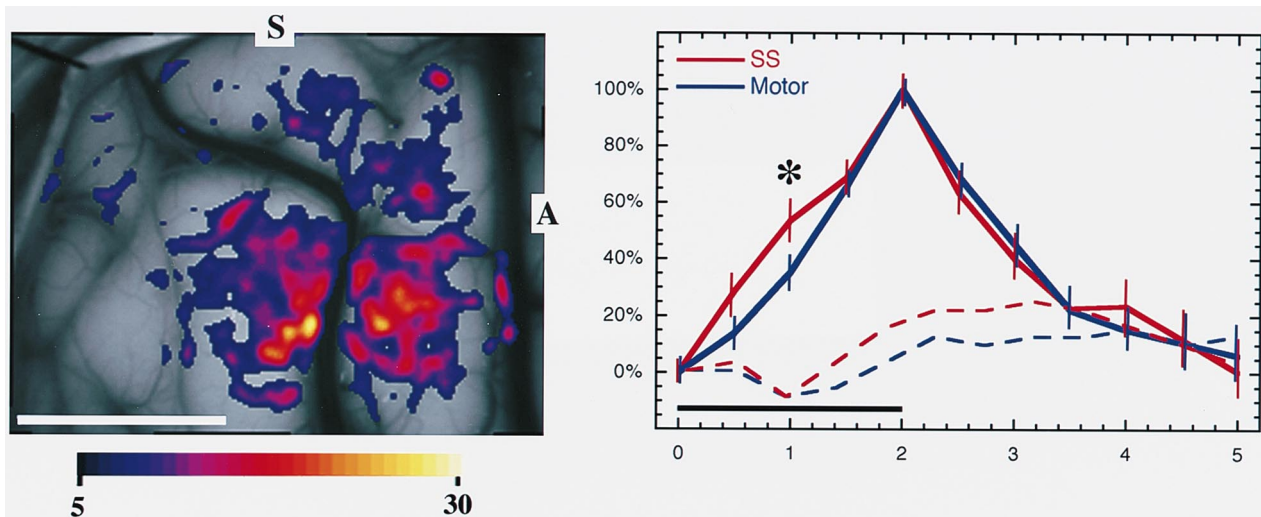


FIG. 3. The temporal specificity of iOIS vibratory optical response. Optical responses were recorded (15 stimulation trials) over exposed pre- and post-central gyrus. Vibratory stimulation was provided by a 110 Hz finger vibrator positioned on the tip of the index finger. Images were acquired every 500 ms and warped into register utilizing an automated image registration algorithm. Optical response began at a pre-stimulus baseline, initiated within 500 ms, rose to peak at 2.0 s, and returned to baseline by 5.0 s. Response over somatosensory cortex preceded motor response. At 500 ms post-stimulation onset, somatosensory responses attained 30% change from baseline, in contrast to 10% over motor cortex. Both pre- and post-central responses peaked by 2.0 s and diminished at the same rate. The intensity difference at 1.0 s (*) was statistically significant ($p < 0.05$, one-sided), and approached significance ($p < 0.10$, one-sided) at 0.5 s. Dashed lines are non-stimulated interleaved controls. Horizontal bar indicates stimulus duration. Error bars are 95% confidence intervals. Control error bars varied from 8 to 15% and always overlapped. Left color bar indicates reflectance change $\times 10^{-4}$. Scale bar is 1 cm. Spatial resolution is $175 \mu\text{m}/\text{pixel}$. A, anterior; S, superior.

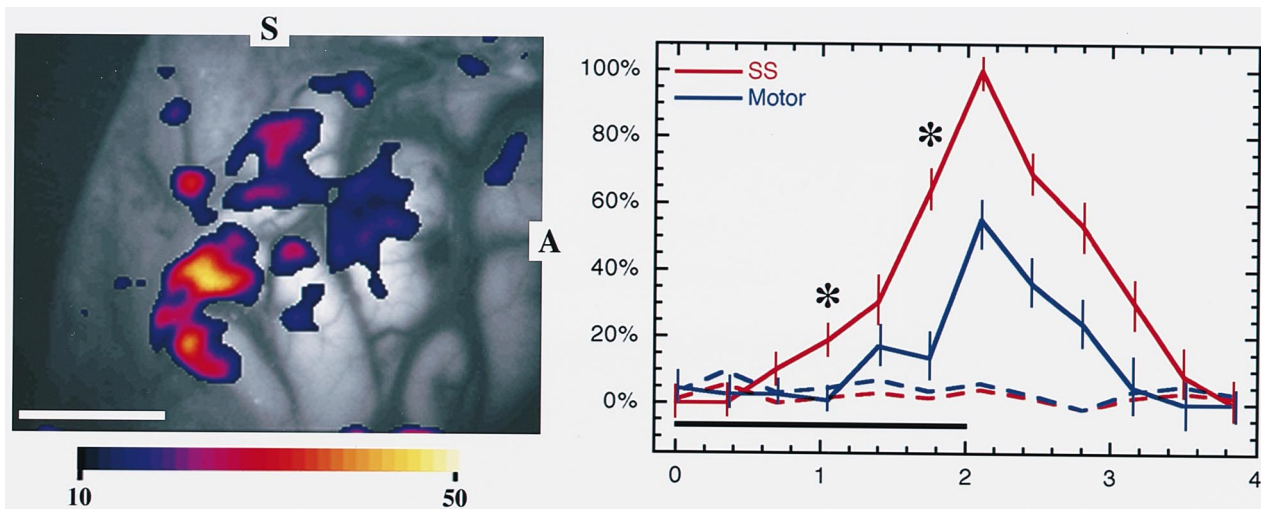


FIG. 4. 350ms temporal specificity of iOIS vibratory optical response. Optical responses were recorded (20 stimulation trials) over exposed pre and post-central gyrus. Vibratory stimulation was provided by a 110Hz finger vibrator positioned on the tip of the index finger. Images were acquired every 350ms and warped into register utilizing an automated image registration algorithm. Optical response began at a pre-stimulus baseline, initiated within 700ms, rose to peak at 2.1s, and returned to baseline by 4.0s. Response over somatosensory cortex preceded motor response. First detectable motor cortex optical responses were at 1.4s, in contrast to 700ms over sensory cortex. Both pre-and post-central responses peaked by 2.1s and diminished at the same rate. Sensory response intensity was near double motor cortex responses. When normalized for peak intensity differences, the intensity difference at 1.05s and 1.75s were statistically significant (* $p < 0.04$ and $p < 0.01$, one-sided, respectively). After normalization the response profiles did not demonstrate temporal specificity after peak response. Dashed lines are non-stimulated interleaved controls. Horizontal bar indicates stimulus duration. Error bars are 95% confidence intervals. Control error bars varied from 5 to 12% and always overlapped. Left color bar indicates reflectance change $\times 10^{-4}$. Scale bar is 1cm. Spatial resolution is $250 \mu\text{m}/\text{pixel}$. A, anterior S, superior.

peak activation for the middle finger. Overlapping regions of cortical response have been observed by previous electrical mapping studies.^{22,25} However, spatial patterns existing within overlapping regions were not described. Interestingly, these individual peak iOIS responses corresponded to cortical regions with large potential changes during transcutaneous median nerve stimulation (Fig. 1). Many of these overlapping optical signals may therefore result from activation of neighboring cortical representations and corresponding regions of peak response. The additional optical signals found outside of these peak regions may correlate with activity producing smaller evoked potential changes and/or result from the overspill of vascular responses observed by utilizing a predominantly perfusion-based method.¹¹ The wavelength utilized in this study (610 nm) is most sensitive to hemodynamic changes (including blood volume) and contains large contributions from hemoglobin oximetry changes.^{10,13} Overlapping signals due to vascular overspill could result from commonly activated branches of the rolandic vessels within the central sulcus.

The observed spatial patterns characterize the relationship between perfusion and electrically based cortical maps. iOIS maps correspond to known cortical functional architecture (superior genu localization for hand,²¹ superior-inferior orientation for middle, index, thumb and face),¹⁷ suggesting perfusion responses accurately reflect the pattern of brain activity. However, novel patterns were observed in perfusion response overlap. These overlapping patterns are not indicated by traditional cortical somatotopy (i.e. the homunculus) and therefore may indicate oversimplification resulting from ESM mapping. ESM mapping often is restricted by patient reported sensations or physical movements (sensory and motor cortex, respectively) associated with cortical stimulation, while iOIS maps reflect cascading processes associated with activity. Alternatively, the iOIS response overlap may indicate 'loose' spatial coupling between perfusion response and underlying electrical activity. Electroencephalographic studies, however, have revealed digit overlap,²² suggesting the iOIS overlapping patterns are not solely due to perfusion/activity mismatch. Thus, peak iOIS responses may represent traditional localizations as observed by electrical maps, while overlapping patterns may reflect the cortical receptive field characteristics and integrative cortical processing.

Temporal specificity: Separate examination of sensory and motor cortices revealed temporal specificity between activated cortex. As shown in Fig. 3, we observed a 20% difference between sensory

(30% at 500 ms) and motor (10% at 500 ms) cortices during early perfusion responses. A statistical significant difference was observed at 1.0 s and approached significance at 500 ms. Figure 3 shows that initial motor cortex responses were delayed 700 ms (at 1.4 s) after detection of sensory responses (at 700 ms). When normalized for intensity differences, a response delay was still evident at 1.75s (64% sensory response, 25% motor response). Statistical significance (at 1.05 s and 1.75 s) also was observed when normalized for intensity. Extensive SSEP studies indicate that both short- and long-latency EPs are generated from somatosensory areas 1 and 3b lying over the crest and within the central sulcus, respectively.²⁶ Motor cortex has not been implicated in these responses. However, increases in pre-central gyrus root mean square (RMS) voltage has been observed in the 40–108 ms latency range. These long-latency changes may reflect activity in area 4.^{27–29} In our study, the pre/post-central gyrus time course differences evident in Figs 3 and 4 may therefore relate to temporal activity differences between sensory and motor cortices (20–80 ms). This study suggests 20–80 ms delays in electrical activity may be communicated in early (500–1750 ms) perfusion-dependent cortical signals. Additionally, Figs 2 and 3 indicate that these early temporal patterns also may be detected either in the absence or presence of response magnitude differences.

The optical time course reported here and in previous studies^{7–9} is consistent with those reported with other perfusion-dependent techniques such as fMRI,^{30,31} TCD⁵ and LDF.⁶ High temporal resolution fMRI studies over motor cortex have indicated 'instantaneous' signal changes (320–640 ms) following an auditory cue.³² LDF has provided rapid capillary flow changes within 100 ms post-stimulation.⁶ In the present study, the initial somatosensory signals (at 0.5 s and 0.7 s in Figs 3 and 4, respectively) localized over cortical tissue, suggesting large vascular branches did not contribute to initial 500 ms responses. Since optical intrinsic signals are closely related to blood volume changes,¹¹ the optical changes (in Figs 3 and 4), occurring within 500 ms post-stimulation may reflect fast capillary flow changes observed by LDF and rapid T2* changes in blood oxygen level dependent (BOLD) fMRI.^{31,33} The early perfusion response differences therefore may be detected utilizing other perfusion dependent methods.

This is the first report of temporal specificity communicated in perfusion signals. The observed temporal patterns match those predicted based on known electrical changes (i.e. primary sensory activity and subsequent secondary motor activations),^{27–29} and therefore suggests that early perfusion response

differences may reflect sequential brain activity. This early perfusion specificity may have significant implications for future functional imaging studies. If imaging modalities possess similar sensitivities, sequential physiological activation of different brain regions may be imaged by monitoring early perfusion response over gray matter (similar to Ref. 32). These differences may also be clinically useful, providing an additional means to identify sensorimotor and other sequentially coupled active cortices.

Conclusion

Perfusion responses provided topographical specificity consistent with previous reports (direct cortical stimulations and electrocorticography); however, only peak perfusion responses provided unique, non-overlapping cortical brain maps. Non-peak signals were more dispersed and produced overlapping responses from different digits. Peak responses correlated well with ESM and EP mapping. Temporally, we observed statistically significant specificity during early optical signals (500–1750 ms), but later perfusion responses were non-specific. Overall, optical measures yielded highly specific, continuous brain maps with very high temporal (350 ms) and spatial resolution (50–80 μm). These results begin to characterize the coupling between brain activity and functional perfusion related cortical signals, and particularly detail the interrelationship between these and electrical brain maps.

References

1. Kwong KK, Belliveau JW, Chesler DA *et al.* *Proc Natl Acad Sci USA* **89**, 5675–5679 (1992).
2. Hurtig RR, Hichwa RD, O'Leary DS *et al.* *J Cerebr Blood Flow Metab* **14**, 423–430 (1994).
3. Grinvald A, Lieke E, Frostig RD *et al.* *Nature* **324**, 361–364 (1986).
4. Villringer A, Planck J, Hock C *et al.* *Neurosci Lett* **154**, 101–4 (1993).
5. Sitzer M, Knorr U and Seitz R. *J Appl Physiol* **77**, 2804–2811 (1994).
6. Lindauer U, Villringer A and Dirnagl U. *Am Physiol Soc* **264**, H1223–H1228 (1993).
7. Haglund MM, Ojemann GA and Hochman DW. *Nature* **358**, 668–671 (1992).
8. Toga AW, Cannestra AF and Black KL. *Cerebr Cortex* **5**, 561–565 (1995).
9. Cannestra AF, Blood AJ, Black KL and Toga AW. *NeuroImage* **3**, 202–208 (1996).
10. Frostig RD, Lieke EE, Ts'o DY and Grinvald A. *Proc Natl Acad Sci USA* **87**, 6082–6086 (1990).
11. Narayan SM, Esfahani P, Blood AJ *et al.* *J Cerebr Blood Flow Metab* **15**, 754–765 (1995).
12. Holthoff K and Witte OW. *J Neurosci* **16**, 2740–2749 (1996).
13. Malonek D and Grinvald A. *Science* **272**, 551–554 (1996).
14. LeManna JC, Sick TJ, Pirarsky SM and Rosenthal M. *Am Physiol Soc* **253**, C477–C483 (1987).
15. Ngai AC, Ko KR, Morii S and Winn HR. *Am J Physiol* **254**, H133–9 (1988).
16. Ngai AC, Meno JR and Winn HR. *J Cerebr Blood Flow Metab* **15**, 124–127 (1995).
17. Penfield W and Rasmussen T. *The Cerebral Cortex of Man: A Clinical Study of Localization of Function*. New York: Macmillan (1950).
18. Nuwer MR, Banoczi WR, Cloughesy TF *et al.* *Brain Topogr* **5**, 53–58 (1992).
19. Woods RP, Grafton ST, Holmes CJ *et al.* *J Comp Assist Tomogr* **22**, 139–152 (1998).
20. Woods RP, Grafton ST, Watson JDG *et al.* *J Comp Assist Tomogr* **22**, 153–165 (1998).
21. Wood CC, Spencer DD, Allison T *et al.* *J Neurosurg* **68**, 99–111 (1988).
22. Baumgartner C, Doppelbauer A, Sutherling WW *et al.* *Electroencephalogr Clin Neurophysiol* **88**, 271–279 (1993).
23. Rumeau C, Tzourio N, Murayama N *et al.* *Am J Neuroradiol* **15**, 567–572 (1994).
24. Sutherling WW, Leveaque MF and Baumgartner C. *Neurology* **42**, 1020–1028 (1992).
25. Rossini PM, Martino G, Narici L *et al.* *Brain Res* **642**, 169–177 (1994).
26. Allison T, McCarthy G, Wood CC *et al.* *J Neurophysiol* **62**, 694–710 (1989).
27. Allison T, McCarthy G, Wood CC *et al.* *J Neurophysiol* **62**, 711–722 (1989).
28. Goldring S, Aras E and Weber PC. *Electroencephalogr Clin Neurophysiol* **29**, 537–550 (1970).
29. Stor PE and Goldring S. *J Neurosurg* **31**, 117–127 (1969).
30. Hemmeke TA, Yetkin FZ, Mueller WM *et al.* *Neurosurgery* **35**, 677–681 (1994).
31. Menon RS, Ogawa S, Xiaoping H *et al.* *Magn Reson Med* **33**, 453–459 (1995).
32. Wiener E, Schad LR, Baudendistel KT *et al.* *Magn Reson Imaging* **14**, 477–483 (1996).
33. Malonek D, Dirnagl U, Lindauer U *et al.* *Proc Natl Acad Sci USA* **94**, 14826–14831 (1997).

ACKNOWLEDGEMENTS: The authors would like to thank Andrew Lee for his artistic and digital creativity. We would also thank the surgical team for their willingness and cooperation. AFC is supported in part by the Training Program in Neuroimaging (MH19950). Additional support provided by research grants to AWT (NIMH MH52083 and NCRR RR05956).

Received 6 May 1998;
accepted 19 May 1998